Coherent reflectance in a system of random Mie scatterers and its relation to the effective-medium approach

Rubén G. Barrera

Instituto de Física, Universidad Nacional Autónoma de México, Apartado Postal 20-364, 01000 México D. F., México

Augusto García-Valenzuela

Centro de Ciencias Aplicadas y Desarrollo Tecnológico, Universidad Nacional Autónoma de México, Apartado Postal 70-186, 04510 México D. F., México

Received February 26, 2002; revised manuscript received October 1, 2002; accepted October 2, 2002

We consider the coherent reflection and transmission of electromagnetic waves from a slab of a dilute system of randomly located, polarizable, spherical particles. We focus our attention on the case where the size of the spheres is comparable to the wavelength of the incident radiation. First, using wave-scattering and Mie theories, we derive expressions for the coherent fields that are transmitted and reflected by a very thin slab. Then we find the effective-current distribution that would act as a source of these fields. We conclude that if the effective currents were induced in an effective medium, this medium must possess, besides an effective electric permittivity, also an effective magnetic permeability. We find that both of these optical coefficients become functions of the angle of incidence and the polarization of the incident wave. Then we calculate the reflection coefficient of a half-space by considering a semi-infinite pile of thin slabs and compare the result with Fresnel relations. Numerical results are presented for the optical coefficients as well as for the half-space reflectance as a function of several parameters. The reflectance is compared with that obtained without considering the magnetic response. Finally, we discuss the relevance and the physics behind our results and indicate as well the measurements that could be performed to obtain an experimental verification of our theory.

OCIS codes: 030.1670, 120.5700, 160.4760, 290.4210, 290.5850, 290.7850.

1. INTRODUCTION

The description and understanding of the propagation of light through random media has attracted the attention of many researchers since the beginning of electrodynamics. One of the first studies on the subject was written by Rayleigh as early as 1899.[1] Here we will deal with the optical properties of granular systems consisting of well-defined isolated inclusions embedded randomly in an otherwise homogeneous matrix. We will assume that in the absence of inclusions the propagation of light in the matrix is well described by the laws of continuum electrodynamics (CE). When an incident beam enters the system, the scattering of light at each of the randomly located inclusions gives rise to a propagating field that can be split into an average and a fluctuating component. The average component is usually called the coherent field and the fluctuating one the diffuse field. In the case where the inclusions are much smaller than the wavelength of light, the power carried by the diffuse component is small compared with that carried by the average component, and sometimes it can be neglected. This is the case, for example, in CE where the atoms and molecules of the material can be regarded as inclusions in vacuum and the diffuse component is completely neglected. Thus the full description of the electromagnetic phenomena is given only in terms of the average (also called macroscopic) fields. In CE the behavior of the average fields is determined through the optical coefficients of the material: the dielectric response ϵ, the magnetic susceptibility μ, and the index of refraction $n = (\epsilon\mu)^{1/2}$, which are continuous functions of space within the volume of the material. This is the meaning of the word "continuous" when one says that in CE the materials can be regarded as continuous.

In the case of granular composite materials in which the inclusions are of macroscopic size but still much smaller than the wavelength of the incident radiation, the behavior of the average electromagnetic fields can be described using the so called effective optical coefficients, which are continuous functions of space within the volume of the composite material. Thus they can be interpreted as the corresponding coefficients of an equivalent, homogeneous, fictitious medium called the effective medium. The theories whose purpose is to determine the relationship between the effective optical properties of the granular system, the optical properties of the constituents, and the geometrical properties of the mixture are called effective-medium theories (EMTs). Whenever these effective properties can be safely used in CE as the corresponding ones of a homogeneous medium, the theories are called unrestricted.[2] The term restricted is reserved for EMTs, in which this is not the case.

1084-7529/2003/020296-16$15.00

Since the seminal work of J. C. Maxwell Garnett[3] in 1904, there has been an intense activity toward the construction of EMTs in granular materials. This activity has been largely concentrated on the case in which the linear dimensions of the inclusions are much smaller than the wavelength of the incident radiation.[4–7] Typical examples of EMTs are those of Maxwell Garnett[3] and Bruggeman.[8] It has also been recognized that an EMT should be constructed differently for materials with different microstructures. For example, while the theory of Maxwell Garnett is adequate for materials with well-defined separate inclusions (granular topology), the theory of Bruggeman turns out to be adequate for materials with intermixed components (aggregate topology). Now since the EMTs do not consider the diffuse component of the fields, they give only a partial description of the full electromagnetic phenomena, and even in cases when the power carried by the diffuse fields might still be small compared with that carried by the coherent fields, one may not neglect it, as for example in the calculation of quantities such as energy dissipation.

An interesting and challenging problem is the extension of these EMTs to the case in which the size of the inclusions is of the same order of magnitude as or even larger than the wavelength of the incident radiation (large inclusions). These theories are known as extended effective-medium theories (EEMTs). In this situation the power carried by the diffuse field may be as large as and sometimes even larger than that carried by the coherent component. The problem now is to determine for these type of systems (with large inclusions) if it is possible to define an effective medium which could be used in CE to describe the propagation of the coherent fields.

There have been several attempts to construct EEMTs. The simplest derivation of the effective index of refraction of a dilute system of randomly located spheres is perhaps that due to van de Hulst.[9] He calculated the coherent superposition of the scattered waves by a dilute ensemble of identical particles located at random within a slab, then compared the transmitted field with the one transmitted by a homogeneous slab of the same width. The contribution of the spheres to the effective index of refraction turns out to be proportional to the filling fraction of spheres times the scattering amplitude in the forward direction. A similar derivation of this result can be also found in the book of Bohren and Huffman.[10] This result is supposed to hold even for systems with large inclusions. There have also been attempts to extend this result to systems with a larger concentration of inclusions[11–15] following as a guide the conceptual procedure used in the theories of Maxwell Garnett[3] and Bruggeman.[8] One of the main ideas in these EEMTs is to replace the quasi-static, dipolar electric polarizability that appears in the case of small spherical inclusions by a dynamical one taken from Mie theory. It turns out that the magnetic dipole resulting from the induced eddy currents within the spherical inclusions also contributes to the dynamic electric polarizability, leading to an additional absorption of energy. The inclusion of a corresponding magnetic dipolar susceptibility has also been considered, and Grimes and Grimes[15] have argued that both the dynamic electric and magnetic polarizabilities are related in such a way that even in the case in which both the matrix and the inclusions are nonmagnetic, the composite system may acquire an effective magnetic susceptibility slightly different from that of vacuum. The main restriction on the validity of all these EEMTs is still that they hold only when the size of the inclusions is small with respect to the wavelength of the incident radiation. There have also been criticisms regarding the internal consistency of these EEMTs and Ruppin[2] has recently reported a thorough analysis on that subject.

In 1986 Bohren used standard wave-scattering theory to calculate the normally reflected and transmitted fields from a composite slab with randomly located inclusions.[16] He noted that even in the dilute limit, if one wants to reproduce these results using an effective medium and CE, one must assume for the case of large inclusions two different indices of refraction: one for reflection, the other for transmission. Instead of accepting this uncomfortable situation he proposed to use two different independent quantities: an effective dielectric response ϵ_{eff} and an effective magnetic susceptibility μ_{eff}. In this way he was able to fulfill the boundary conditions and properly recover the reflection and transmission amplitudes given by wave-scattering theory. Nevertheless, the physical basis of the magnetic behavior of a composite consisting of a mixture of nonmagnetic components was not completely clear, and he was hesitant to consider the concept of an effective medium for the case of a system with large inclusions. There were also explicit criticisms[17] of the notion of attributing an effective magnetic susceptibility to a composite with nonmagnetic constituents, the critics arguing that it might simply be a mathematical trick used to fulfill boundary conditions but void of any physical significance.

Looking now at the problem of wave propagation through a system of randomly located inclusions within a more formal theoretical framework, and without invoking the idea of an effective medium, one realizes that there has also been an intense and prolific activity in searching for the solution to this problem by the use of analytic wave theory of multiple scattering. The mathematical procedures that have mostly been used to solve the electromagnetic multiple-scattering equations constituting this problem are the T-matrix formalism and the integral-equation formulation of Maxwell's equations involving N-particle Green's function. The results obtained so far have become especially important in applications to remote sensing in the microwave region[18] and to astrophysics, concerning radiation transfer in planetary atmospheres. For the case of finite clusters of spheres these mathematical procedures yield exact results.

Analytical wave theory of multiple scattering provides a formal procedure to calculate the coherent component of the electromagnetic field propagating in a medium of random scatterers through the solution of a hierarchy of multiple-scattering equations. These equations can be solved with various degrees of approximation.[19–22] Truncation at the first stage in the hierarchy of equations, known as the effective-field approximation, was used by Foldy[23] and Lax[24,25] to derive the effective wave vector and the corresponding effective index of refraction for waves propagating in the bulk of the random system of discrete scatterers. To linear order in the filling fraction of spheres, their result turned out to be the same as the one of van de Hulst.[9] At this stage one could perform a conceptual leap and interpret this effective index of refraction as a property of an effective medium and then ask whether its use is unrestricted, that is, whether one could use it together with CE to calculate other optical properties such as the reflection and transmission amplitudes of the coherent field at the interface of a half-space of randomly located scatterers, succinctly called coherent-reflection and transmission amplitudes. Obviously this problem is not well posed, because the use of CE would rely on Fresnel relations, and Fresnel relations would require, besides the effective index of refraction n_{eff}, an effective dielectric response ϵ_{eff} and an effective magnetic susceptibility μ_{eff} independently. What has usually been assumed in a system with nonmagnetic components is to take the effective magnetic susceptibility μ_{eff} equal to the one in vacuum μ_0 and then use n_{eff} as unrestricted. But this assumption has never been proved and it would require the independent calculation of the effective dielectric and magnetic responses regarded as the relation between the induced effective currents and the average fields. Furthermore even if this calculation could be accomplished and the determination of the reflection and transmission amplitudes could finally be made using Fresnel relations, it would be still necessary to check that the results so obtained are consistent with an independent calculation of the same reflection and transmission amplitudes using for example standard wave-scattering theory. Our objective here is precisely to give an answer to these questions using a rather intuitive approach.

First we use standard wave-scattering theory to calculate the coherent component of the fields radiated by a thin slab of randomly located identical, polarizable, nonmagnetic spheres when driven by a plane wave incident at an arbitrary angle and in the dilute limit. Then we find the currents that would act as the sources of these radiated fields and identify them as the induced effective currents, that is, the currents induced in an effective medium. We find that these effective currents have to have a component coming from closed currents, which we identify as closed currents induced in the spheres by the time variations of the incident magnetic field, thus giving rise to a true magnetic response. Then we take account, in an average way, of multiple-scattering effects by constructing a half-space as a pile of slabs and solving the transfer equations for the coherent fields. By this procedure we calculate the coherent-reflection and transmission amplitudes of the half-space. Although these results are valuable by themselves, independently of any relation to the concept of an effective medium, we also use them to corroborate that the results so obtained are consistent with CE and the concept of an effective medium only if the effective medium possesses, besides an effective dielectric response ϵ_{eff}, also an effective magnetic susceptibility μ_{eff}. The expressions derived for the dielectric and magnetic responses ϵ_{eff} and μ_{eff} depend on the angle of incidence and the polarization of the incident beam, but the effective index of refraction $n_{\text{eff}} = (\epsilon_{\text{eff}}\mu_{\text{eff}})^{1/2}$ turns out to be equal to the one derived by van de Hulst. Therefore the resulting EEMT becomes of the restricted type.

Finally we provide numerical calculations which could be used to test experimentally the validity of our results concerning the coherent reflectance of a half-space compared with the corresponding results coming from the unrestricted use in CE of the effective refractive index derived by van de Hulst. In comparing against experiments, the interpretation of our results as coming from an effective medium with an anisotropic magnetic response is absolutely optional because, as pointed out above, our results do not depend on such an interpretation. Furthermore our work fulfills another objective by helping to understand physically the magnetic properties at optical frequencies of an effective medium within a restricted EEMT for large inclusions and nonnormal incidence.

The paper is structured as follows. In Section 2 we calculate the coherent transmission and reflection from a thin slab of a random system of spheres. In Section 3 we derive the effective optical coefficients of an equivalent homogeneous medium by identifying the sources of the radiated fields as open and closed currents induced in the effective medium, and give some numerical examples. In Section 4 we derive the coherent-reflection amplitude for a half-space built up as a pile of slabs and compare our results with Fresnel relations to identify the electromagnetic properties of an equivalent effective medium. We give some numerical examples and discuss the corresponding formulas for a system of particles embedded in a homogeneous matrix. In Section 5 we provide a discussion of the results and our conclusions.

2. COHERENT TRANSMISSION AND REFLECTION FROM A THIN SLAB

We consider a dilute, random distribution of spherical particles in vacuum (no matrix) contained in a boundless slab region parallel to the $x-y$ plane with $-d/2 < z < d/2$. The system is in the presence of an incident plane wave with an electric field given by

$$\mathbf{E}^i(\mathbf{r}, t) = E_0 \exp[i(\mathbf{k}^i \cdot \mathbf{r} - \omega t)]\hat{\mathbf{e}}_i, \tag{1}$$

where $\mathbf{r}$ and t are the position vector and time, respectively, ω is the radial frequency, $\hat{\mathbf{e}}_i$ is a unit vector in the direction of polarization, $\mathbf{k}^i = k_y^i\hat{\mathbf{a}}_y + k_z^i\hat{\mathbf{a}}_z$ is the incident wave vector assumed to lie in the $y-z$ plane, and $\hat{\mathbf{a}}_x$, $\hat{\mathbf{a}}_y$, and $\hat{\mathbf{a}}_z$ are unit vectors along the Cartesian axes of coordinates (see Fig. 1). The electric field satisfies $\hat{\mathbf{e}}_i \cdot \mathbf{k}^i = 0$ and $|\mathbf{k}^i| = k$, where $k = \omega/c = 2\pi/\lambda$ is the wave number in vacuum, λ is the corresponding wavelength, and c is the speed of light. The time dependence $\exp(-i\omega t)$ will be assumed throughout the paper and will not be shown hereafter. We will be using SI units.

The incident field is scattered by the particles, and we assume their number density is low enough that the single-scattering approximation is valid. This means that the field exiting each particle is the incident field; we neglect the contribution coming from the field scattered by all other particles. The scattered field $\mathbf{E}^S$ due to a col-

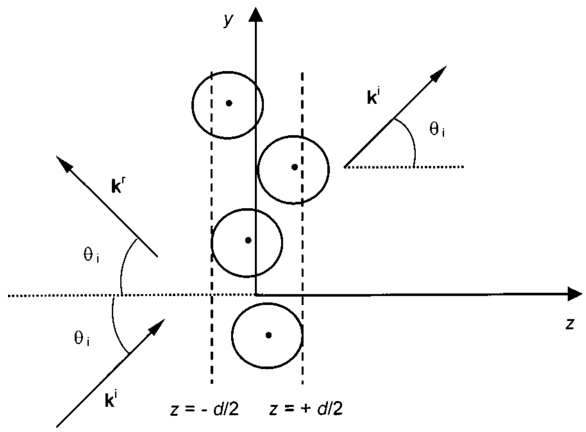

Fig. 1. Slab of a dilute random system of spheres. The centers of the particles are within the planes $z = -d/2$ and $z = d/2$.

lection of N spherical particles with their centers located at $\{\mathbf{r}_1, \mathbf{r}_2, \ldots, \mathbf{r}_p, \ldots, \mathbf{r}_N\}$ can be written as[26]

$$\mathbf{E}^S(\mathbf{r}) = \sum_{p=1}^{N} \int \mathrm{d}^3 r' \int \mathrm{d}^3 r'' \bar{\bar{G}}_0(\mathbf{r}, \mathbf{r}') \cdot \bar{\bar{T}}(\mathbf{r}' - \mathbf{r}_p, \mathbf{r}'' - \mathbf{r}_p) \cdot \mathbf{E}^i(\mathbf{r}''), \tag{2}$$

where $\bar{\bar{G}}_0(\mathbf{r}, \mathbf{r}')$ is the dyadic Green's function in free space, $\bar{\bar{T}}(\mathbf{r}', \mathbf{r}'')$ is the transition operator for a sphere, and $\mathbf{E}^i$ denotes the incident field. To deal with a slab geometry it is convenient to work in a plane-wave representation, so we substitute the plane-wave expansion of the dyadic Green's function

$$\bar{\bar{G}}_0(\mathbf{r}, \mathbf{r}') = \frac{i}{8\pi^2} \iint \mathrm{d}k_x^s \mathrm{d}k_y^s \frac{1}{k_z^s} (\bar{\bar{\mathbf{1}}} - \hat{\mathbf{k}}_\pm^s \hat{\mathbf{k}}_\pm^s) \exp[i\mathbf{k}_\pm^s \cdot (\mathbf{r} - \mathbf{r}')] \tag{3}$$

valid in the region outside the particle ($r > r'$), the momentum representation of the transition operator

$$\bar{\bar{T}}(\mathbf{r}' - \mathbf{r}_p, \mathbf{r}'' - \mathbf{r}_p) = \frac{1}{(2\pi)^6} \int \mathrm{d}^3 p' \int \mathrm{d}^3 p'' \exp[i\mathbf{p}' \cdot (\mathbf{r}' - \mathbf{r}_p)] \bar{\bar{T}}(\mathbf{p}', \mathbf{p}'') \times \exp[-i\mathbf{p}'' \cdot (\mathbf{r}'' - \mathbf{r}_p)], \tag{4}$$

and the plane-wave expression of the incident field into Eq. (2) to get

$$\mathbf{E}^S(\mathbf{r}) = \frac{i}{8\pi^2} E_0 \sum_{p=1}^{N} \iint \mathrm{d}k_x^s \mathrm{d}k_y^s \frac{(\bar{\bar{\mathbf{1}}} - \hat{\mathbf{k}}_\pm^s \hat{\mathbf{k}}_\pm^s)}{k_z^s} \cdot \bar{\bar{T}}(\mathbf{k}_\pm^s, \mathbf{k}^i) \cdot \hat{\mathbf{e}}_i \exp[-i(\mathbf{k}_\pm^s - \mathbf{k}^i) \cdot \mathbf{r}_p] \times \exp(i\mathbf{k}_\pm^s \cdot \mathbf{r}). \tag{5}$$

Here $\mathbf{k}_\pm^s = k_x^s \hat{\mathbf{a}}_x + k_y^s \hat{\mathbf{a}}_y \pm k_z^s \hat{\mathbf{a}}_z$, $k_z^s = [k^2 - (k_x^s)^2 - (k_y^s)^2]^{1/2}$, and $\bar{\bar{T}}(\mathbf{p}', \mathbf{p}'')$ is the momentum representation of the transition operator $\bar{\bar{T}}(\mathbf{r}', \mathbf{r}'')$ of an isolated sphere. This is the plane-wave expansion of the scattered field, meaning that the scattered field is expressed as a sum of plane waves propagating along the $\mathbf{k}_\pm^s$ directions; the signs $\pm$ refer to the field propagating to the right (+) and to the left (−) of each particle. The factor $\exp[-i(\mathbf{k}_\pm^s - \mathbf{k}^i) \cdot \mathbf{r}_p]$ keeps track of the phase difference of the field scattered by different particles.

Notice that the arguments of $\bar{\bar{T}}$ run over all possible values of k_x^s and k_y^s. But here we are interested only in the coherent component of this radiated field, so we perform the configurational average of $\mathbf{E}^S$ over a slab of width d comprised between the planes $z = -d/2$ and $z = +d/2$. In the averaging procedure we will further assume that the positions of the particles are independent of each other (i.e., we ignore the exclusion volume) and that the probability of finding a particle with its center inside the volume $\mathrm{d}^3\mathbf{r}$ is uniform and given by $\mathrm{d}^3\mathbf{r}/V$, where V is the volume of the slab. Therefore the configurational average of $\mathbf{E}^S$ is calculated by integrating, in the expression given by Eq. (5), the location of each particle $\mathrm{d}^3\mathbf{r}_p$ over the volume of the slab, keeping $N/V \equiv \rho$ constant. The integrals over $\mathrm{d}x_p$ and $\mathrm{d}y_p$ yield delta functions $\delta(k_x^s - k_x^i)$ and $\delta(k_y^s - k_y^i)$ and the integral over $\mathrm{d}z_p$ is performed from $-d/2$ to $+d/2$. We obtain

$$\langle \mathbf{E}^S(\mathbf{r}) \rangle_{\mathrm{slab}} = \begin{cases} \mathbf{E}_+^S \exp(i\mathbf{k}^i \cdot \mathbf{r}) & \text{for } z > d/2 \\ \mathbf{E}_-^S \exp(i\mathbf{k}^r \cdot \mathbf{r}) & \text{for } z < -d/2 \end{cases}, \tag{6}$$

where

$$\mathbf{E}_+^S = i\frac{E_0}{2}\rho \frac{(\bar{\bar{\mathbf{1}}} - \hat{\mathbf{k}}^i \hat{\mathbf{k}}^i)}{k_z^i} \cdot \bar{\bar{T}}(\mathbf{k}^i, \mathbf{k}^i) \cdot \hat{\mathbf{e}}_i d, \tag{7}$$

$$\mathbf{E}_-^S = i\frac{E_0}{2}\rho \frac{(\bar{\bar{\mathbf{1}}} - \hat{\mathbf{k}}^r \hat{\mathbf{k}}^r)}{k_z^i} \cdot \bar{\bar{T}}(\mathbf{k}^r, \mathbf{k}^i) \cdot \hat{\mathbf{e}}_i \frac{\sin k_z^i d}{k_z^i}. \tag{8}$$

Here $\mathbf{k}^r = k_x^i \hat{\mathbf{a}}_x + k_y^i \hat{\mathbf{a}}_y - k_z^i \hat{\mathbf{a}}_z$ is the wave vector in the specular direction and $k_z^i = [k^2 - (k_x^i)^2 - (k_y^i)^2]^{1/2}$. One can see that for $z > d/2$ the coherent component of the scattered field propagates to the right as a plane wave with its wave vector along the same direction as the incident wave, while for $z < -d/2$ it propagates to the left, also as a plane wave, but with its wave vector along the specular direction. This means that the scattered field interferes constructively along two directions $\mathbf{k}^i$ and $\mathbf{k}^r$ independent of the location of the scatterers. For this reason these are the only components of the field that survive after a configurational average. Also the amplitudes of these plane waves depend solely on the scattering properties of an isolated particle (through $\bar{\bar{T}}$) and are directly proportional to the number of particles (through ρ). This is a manifestation of the single-scattering approximation. Furthermore since both of the arguments of $\bar{\bar{T}}$ in Eqs. (7) and (8) are wave vectors with the same magnitude k^i, one can write $\bar{\bar{T}}$ in terms of the far-field scattering dyad $\bar{\bar{F}}$, defined as

$$\mathbf{E}_{\mathrm{far}}^S(\mathbf{r}) = E_0 \frac{\exp(ikr)}{r} \bar{\bar{F}}(\hat{\mathbf{k}}^s, \hat{\mathbf{k}}^i) \cdot \hat{\mathbf{e}}_i, \tag{9}$$

where $\mathbf{E}_{\mathrm{far}}^S(\mathbf{r})$ is the field scattered in the region far away from a particle centered at the origin; $\hat{\mathbf{k}}^i$ and $\hat{\mathbf{k}}^s$ are the directions of travel of the incident plane wave and the scattered field, respectively; and $\hat{\mathbf{e}}_i$ is the polarization of the incident wave and E_0 its amplitude. It can be shown that the relationship between the transition operator in Eqs. (7) and (8) and the far-field scattering dyad can be written as

$$(\bar{\bar{\mathbf{I}}} - \hat{\mathbf{k}}^i\hat{\mathbf{k}}^i) \cdot \bar{\bar{T}}(\mathbf{k}^i,\mathbf{k}^i) = 4\pi\bar{\bar{F}}(\hat{\mathbf{k}}^i,\hat{\mathbf{k}}^i), \tag{10}$$

$$(\bar{\bar{\mathbf{I}}} - \hat{\mathbf{k}}^r\hat{\mathbf{k}}^r) \cdot \bar{\bar{T}}(\mathbf{k}^r,\mathbf{k}^i) = 4\pi(\hat{\mathbf{k}}^r, \hat{\mathbf{k}}^i). \tag{11}$$

But the incident field and the plane-wave components of the scattered far field are both transverse: $\mathbf{E}^S_{\text{far}}$ and $\mathbf{E}^i$ are perpendicular to $\hat{\mathbf{k}}^s$ and $\hat{\mathbf{k}}^i$, respectively, and $\bar{\bar{F}}(\hat{\mathbf{k}}^s, \hat{\mathbf{k}}^i)$ should relate the two transverse components of the incident field with the two transverse components of the scattered far field. Therefore in an appropriate reference frame $\bar{\bar{F}}(\hat{\mathbf{k}}^s, \hat{\mathbf{k}}^i)$ should have only $2 \times 2 = 4$ different components. These four different components are the components of the so-called scattering matrix. Following Bohren and Huffman[10] we write the relationship between the scattered far field and the incident field as

$$\begin{pmatrix} E^S_{\text{far}\parallel} \\ E^S_{\text{far}\perp} \end{pmatrix} = \frac{\exp(ikr)}{-ikr}\begin{bmatrix} S_2(\theta) & S_4(\theta) \\ S_3(\theta) & S_1(\theta) \end{bmatrix}\begin{pmatrix} E^i_\parallel \\ E^i_\perp \end{pmatrix}, \tag{12}$$

where S_j with $j = 1$ to 4 are the components of the (2×2) scattering matrix and the subindexes $\parallel$ and $\perp$ denote components parallel and perpendicular, respectively, to the scattering plane, which is the plane generated by the incident and scattering wave vectors. For a sphere $S_3(\theta) = S_4(\theta) = 0$, and one can easily show that $\mathbf{E}^S_+$ and $\mathbf{E}^S_-$ in Eqs. (7) and (8) can also be written as

$$\mathbf{E}^S_+ = -E_0\gamma\frac{kd}{\cos\theta_i}S(0)\hat{\mathbf{e}}_i, \tag{13}$$

$$\begin{aligned}\mathbf{E}^S_- = -E_0\gamma\frac{k}{\cos\theta_i}\frac{\sin k^i_z d}{k^i_z} &\times [-(\cos\theta_i\hat{\mathbf{a}}_y + \sin\theta_i\hat{\mathbf{a}}_z)(\cos\theta_i\hat{\mathbf{a}}_y - \sin\theta_i\hat{\mathbf{a}}_z) \\ &\times S_2(\pi - 2\theta_i) + \hat{\mathbf{a}}_x\hat{\mathbf{a}}_x S_1(\pi - 2\theta_i)] \cdot \hat{\mathbf{e}}_i,\end{aligned} \tag{14}$$

where $S(0) \equiv S_1(\theta = 0) = S_2(\theta = 0)$ is called the forward-scattering amplitude, $\gamma \equiv 3f/2x^3$, $x \equiv ka$ is the size parameter, $f = N4\pi a^3/3V$ is the filling fraction of spheres, $\pi - 2\theta_i$ is the specular direction, and we recall that $k^i_z = k\cos\theta_i$. Notice that while $\mathbf{E}^S_+$ is directly proportional to d, $\mathbf{E}^S_-$ is proportional to $\sin k^i_z d/k^i_z$. Here d is the thickness of the averaging region where the centers of the spheres are randomly located. Since we are considering that the slab is thin enough for the single-scattering approximation to be valid, one can take d small enough and approximate $\sin k^i_z d/k^i_z \approx d$, as will be discussed below. Notice also that in general $|\mathbf{E}^S_+| \neq |\mathbf{E}^S_-|$; this is a direct consequence of the forward–backward anisotropy of Mie scattering—that is, $S(0) \neq S_m(\pi - 2\theta_i)$ for $m = 1,2$. We also recall that this anisotropy is more acute the larger the sphere. For spheres whose radii are very small with respect to the incident wavelength, this anisotropy almost disappears and one has $|\mathbf{E}^S_+| \approx |\mathbf{E}^S_-|$.

We now pose the following problem: The incident field induces currents in the spheres within the slab. The sources of the coherent (average) fields radiated by the thin slab and given by Eqs. (6)–(8) and (13)–(14) are the averages of these induced currents. Keeping this in mind, we ask the following:

1. Is it possible to construct a simple model for the average of these induced currents?
2. Is it possible to associate with the thin slab an effective electric or magnetic susceptibility that relates the incoming field to the average of these induced currents?
3. If so, is it then possible to describe the propagation, reflection, and transmission of the average electromagnetic field in a thick slab or a half-space in terms of these effective susceptibilities?
4. Finally, is it possible to identify the actual induction process of the currents in the spheres and the physical nature of the effective susceptibilities?

To answer all these questions and to keep the calculation procedure as clear as possible, we will treat the two polarizations of the incoming beam separately: the TE polarization when $\hat{\mathbf{e}}_i = \hat{\mathbf{a}}_x$, and the TM polarization when $\hat{\mathbf{e}}_i = \cos\theta_i\hat{\mathbf{a}}_y - \sin\theta_i\hat{\mathbf{a}}_z$.

3. EFFECTIVE ELECTRIC PERMITTIVITY AND MAGNETIC PERMEABILITY

In TE polarization ($\hat{\mathbf{e}}_i = \hat{\mathbf{a}}_x$) the amplitudes of the radiated fields $\mathbf{E}^S_+$ and $\mathbf{E}^S_-$ are given by

$$\mathbf{E}^S_+ = -E_0\gamma\frac{kd}{\cos\theta_i}S(0)\hat{\mathbf{a}}_x, \tag{15}$$

$$\mathbf{E}^S_- = -E_0\gamma\frac{k}{\cos\theta_i}\frac{\sin k^i_z d}{k^i_z}S_1(\pi - 2\theta_i)\hat{\mathbf{a}}_x. \tag{16}$$

We seek now to find the effective-current distribution that acts as a source of these fields and identify these effective currents with the average current distribution induced in an effective medium. To model the effective currents within the thin slab, we postulate the simplest possible geometry: a two-dimensional (2D) homogeneous and isotropic sheet with no internal structure. We locate the sheet at the $z = 0$ plane in the presence of an incident plane wave with TE polarization, that is,

$$\mathbf{E}^i(\mathbf{r}, t) = E_0\exp[i(k^i_y y + k^i_z z)]\hat{\mathbf{a}}_x, \tag{17}$$

where $\mathbf{E}^i$ is the incident electric field. Since the incident electric field lies along the x-direction and the sheet is isotropic in the x–y plane, we assume that the effective induced current density also lies along the x-direction and can be written as

$$\mathbf{J} = j_{0x}\delta(z)\exp(ik^i_y y)\hat{\mathbf{a}}_x, \tag{18}$$

where j_{0x} is actually a surface current density and the spatial dependence is the one corresponding to the excitation by the incident plane wave (at $z = 0$). One can easily show that the fields radiated by this current distribution are two plane waves, one traveling to the right ($z > 0$) with wave vector $\mathbf{k}^i$ and one traveling to the left ($z < 0$) with wave vector $\mathbf{k}^r$; that is,

$$\mathbf{E}^J = \begin{cases} \mathbf{E}^J_+\exp(i\mathbf{k}^i \cdot \mathbf{r}) & \text{for } z > 0 \\ \mathbf{E}^J_-\exp(i\mathbf{k}^r \cdot \mathbf{r}) & \text{for } z < 0 \end{cases}, \tag{19}$$

where $\mathbf{k}^i$ and $\mathbf{k}^r$ have the same meaning as in Eq. (6),

$$E^J_{\pm x} = -\frac{1}{2}\mu_0 j_{0x}\frac{\omega}{k^i_z}, \tag{20}$$

and μ_0 is the magnetic permeability of vacuum. These radiated fields are similar to the ones radiated by the slab with spherical inclusions. Nevertheless while here $E^J_{+x} = E^J_{-x}$, in the case of the slab one has a right–left anisotropy; that is $E^S_{+x} \neq E^S_{-x}$, which comes from the anisotropy of Mie scattering and is explicitly displayed in Eqs. (15) and (16). Furthermore, the result $E^J_{+x} = E^J_{-x}$ is a direct consequence of Faraday's law $\nabla \times \mathbf{E} = -i\omega\mathbf{B}$, which demands the continuity of E^J_x whenever B^J_y is finite. Here $\mathbf{B}$ is the magnetic field. Therefore if one wants to find a distribution of induced currents that properly simulates the sources of the fields radiated by the slab of spherical particles, one is forced to conclude that this is not possible with the current distribution proposed in Eq. (18). The fulfillment of Faraday's law requires a singular value of B_y at $z = 0$ as the only way to obtain a right–left anisotropy in the wave amplitudes of the radiated electric field. But the only way to get a singular value of B_y at $z = 0$ would be to have a distribution of closed currents that generate a magnetization $\mathbf{M}$ in the sheet along the y-direction. Only in this manner can $B_y/\mu_0 = H_y + M_y$ have a singular contribution. An average of closed currents running along the x-direction can be written as two surface current densities j_C running in opposite directions, that is,

$$\begin{aligned}\mathbf{J}_C &= \lim_{\varepsilon\to 0} j_C[\delta(z+\varepsilon/2) - \delta(z-\varepsilon/2)]\exp(ik_y y)\hat{\mathbf{a}}_x \\ &= \mathcal{J}_C\delta'(z)\exp(ik^i_y y)\hat{\mathbf{a}}_x,\end{aligned} \tag{21}$$

where the prime indicates spatial derivative and $\mathcal{J}_C$ corresponds to a surface magnetization, as will be shown below. These closed currents should be induced by an electric field generated by the time variations of the magnetic field along the y direction. In a boundless, homogeneous, nonmagnetic sheet, the electric field generated by the time variations of a magnetic field cannot induce any closed currents, but in a slab with spherical inclusions the closed currents can be induced at the inclusions. Therefore one can regard $\mathbf{J}_C$ as the average of the closed currents induced in the spheres. Let us now define the magnetization field $\mathbf{M}$ as

$$\mathbf{J} = \nabla \times \mathbf{M}, \tag{22}$$

where $\mathbf{J}$ is, in general, the average of the closed currents induced in the material. In our case $\mathbf{J}_C$ yields a magnetization in the y-direction, which can be written as

$$\mathbf{M} = m_{0y}\delta(z)\exp(ik^i_y y)\hat{\mathbf{e}}_y, \tag{23}$$

where $m_{0y} = \mathcal{J}_C$ is the surface magnetization. Now one can show that the electric field radiated by this induced magnetization is also in the form of plane waves, as were the ones in Eq. (19), but with amplitudes

$$E^J_{\pm x} = \pm\frac{i}{2}\omega\mu_0 m_{0y}, \tag{24}$$

which are discontinuous at $z = 0$. This discontinuity obviously arises from the discontinuity of the closed-current distribution in Eq. (21). If we now add the fields radiated by the current distributions in Eqs. (18) and (21) we would have, as before, two plane waves propagating along $\mathbf{k}^i$ for $z > 0$ and $\mathbf{k}^r$ for $z < 0$ but with a total electric field given now by

$$E^J_{\pm x} = \tfrac{1}{2}\mu_0\omega\left(-\frac{j_{0x}}{k^i_z} \pm im_{0y}\right), \tag{25}$$

which has a right–left anisotropy. From this we conclude that to simulate the radiation of a thin slab with spherical inclusions one requires as sources, open- and closed-current distributions. Since the closed currents should be induced by the time variations of the magnetic field, the response of the system should be interpreted as an actual and true magnetic response. One can now regard the open and closed current distributions as the response of an effective material to the incoming field. But before going further in trying to identify the electric and magnetic responses of this effective material, we should consider that if H_y can induce closed currents in the sheet, the same should happen with the time variations of H_z. In this case closed currents should be induced in the x–y plane with a corresponding magnetization in the z-direction. Therefore in order to be consistent we should also consider the field radiated by a source such as

$$\mathbf{M} = -m_{0z}\delta(z)\exp(ik^i_y y)\hat{\mathbf{e}}_z. \tag{26}$$

The minus sign comes from the difference in phase between H_y and H_z in TE polarization. It is straightforward to show that the fields radiated by this source are also two plane waves, as in Eq. (19), propagating along $\mathbf{k}^i$ for $z > 0$ and $\mathbf{k}^r$ for $z < 0$, with an amplitude

$$E^J_{\pm x} = \frac{i}{2}\mu_0\omega m_{0z}\frac{k^i_y}{k^i_z}. \tag{27}$$

Note that in this case $H_z = B_z/\mu_0 - m_{0z}\delta(z)\exp(ik^i_y y)$ is singular at $z = 0$. Adding up the contributions to the amplitude of the radiated field of the three sources given by Eqs. (18), (23), and (26), we get

$$E^J_{\pm x} = \frac{1}{2}\mu_0\omega\left(-\frac{j_{0x}}{k^i_z} \pm im_{0y} + im_{0z}\frac{k^i_y}{k^i_z}\right). \tag{28}$$

We will now assume that the averages of the induced currents are proportional to the incident field through some effective response functions, and then try to find the values for which one recovers the fields radiated by the thin slab with spherical inclusions. First we define the polarization field $\mathbf{P}$ as

$$\mathbf{J} = \frac{\partial\mathbf{P}}{\partial t} \to -i\omega\mathbf{P}, \tag{29}$$

where $\mathbf{J}$ is the average of the induced current in the material. Then we define the electric susceptibility tensor $\bar{\bar{\chi}}^E$ as $\mathbf{P} = \epsilon_0\bar{\bar{\chi}}^E \cdot \mathbf{E}$, where $\mathbf{E}$ is the average electric field. In the same manner the magnetic susceptibility tensor $\bar{\bar{\chi}}^H$ is defined as $\mathbf{M} = \bar{\bar{\chi}}^H \cdot \mathbf{H}$, where $\mathbf{H}$ is the average H field. For an object such as the 2D sheet we are dealing with, the description of the response should be given in terms of the corresponding surface susceptibilities—denoted by $\bar{\bar{\chi}}_S^E$ and $\bar{\bar{\chi}}_S^H$—that relate the **E** and the **H** field to the surface polarization and surface magnetization, respectively. We also assume that in our coordinate system $\bar{\bar{\chi}}_S^E$ and $\bar{\bar{\chi}}_S^H$ are diagonal, and can be written as $\bar{\bar{\chi}}_S^E = (\chi_{S\|}^E, \chi_{S\|}^E, \chi_{S\perp}^E)$ and $\bar{\bar{\chi}}_S^H = (\chi_{S\|}^H, \chi_{S\|}^H, \chi_{S\perp}^H)$, where the subindexes $\|$ and $\perp$ denote parallel and perpendicular to the sheet, respectively. The response of the 2D sheet is clearly anisotropic in the $\|$ and $\perp$ directions, but we are regarding the $x-y$ plane as isotropic. Now we assume that the system is so dilute that the average induced current and magnetization distributions in Eqs. (18), (23), and (26) are proportional to the incident field; thus

$$j_{0x} = -i\omega\epsilon_0\chi_{S\|}^E E_0, \tag{30}$$

$$m_{0y} = \chi_{S\|}^H H_0\cos\theta_i = \chi_{S\|}^H\frac{k}{\omega\mu_0}E_0\cos\theta_i, \tag{31}$$

$$m_{0z} = \chi_{S\perp}^B B_0\sin\theta_i = \chi_{S\perp}^B\frac{k}{\omega}E_0\sin\theta_i, \tag{32}$$

where we have used the relations between **E**, **H** and **B** given by Maxwell's equations and we have introduced, in Eq. (32), the surface response $\chi_{S\perp}^B$ to the **B** field instead of the response $\chi_{S\perp}^H$ to the **H** field. We do this because in the case where the magnetization is along the z-direction and given by Eq. (26), the field $H_z = B_z/\mu_0 - m_{0z}\delta(z)\exp(ik_y^i y)$ is singular at $z = 0$, and it is not adequate to define a response to a singular field. On the contrary, the field B_z is continuous and can be regarded as the driving field of the induced magnetization.

Now to get the amplitude of the radiated plane waves $E_{\pm x}^J$ in terms of the surface response functions, we substitute Eqs. (30)–(32) into Eq. (28) to yield

$$E_{\pm x}^J = \frac{i}{2}k\left(\frac{\chi_{S\|}^E}{\cos\theta_i} \pm \chi_{S\|}^H\cos\theta_i + \mu_0\chi_{S\perp}^B\frac{\sin^2\theta_i}{\cos\theta_i}\right)E_0. \tag{33}$$

We now compare the amplitudes of the waves radiated by this sheet, characterized by three effective surface response functions, with the amplitudes of the waves radiated by the slab with spherical inclusions. To do this we first imagine that the effective response of the sheet is actually describing the response of a slab of a finite width d. One can regard the sheet as the shape at the end of a limiting process which starts with a slab of a finite width. For example one can define the surface susceptibility $\chi_{S\|}^E$ as $\chi_{S\|}^E = \lim_{d\to 0}\chi^E d$, where χ^E is the bulk susceptibility of a homogeneous and isotropic slab. Therefore before we compare the amplitudes of the waves radiated by the sheet and given by Eq. (33) with the corresponding ones of a slab of width d with randomly located spheres and given by Eqs. (15) and (16), we have to perform in Eq. (33) the following replacements:

$$\chi_{S\|}^E \to \chi^E d, \tag{34}$$

$$\chi_{S\|}^H \to \chi^H d, \tag{35}$$

where χ^H is the bulk magnetic susceptibility of a homogeneous and isotropic slab and

$$\chi_{S\perp}^B \to \frac{\chi^H d}{\mu} \approx \frac{\chi^H d}{\mu_0}. \tag{36}$$

In this last replacement we are taking into account that in the $\perp$ direction there is a surface magnetization at the two parallel faces of the slab that produces a difference between the average **B** and **H** fields. This does not happen along the $\|$ direction because along this direction the system is boundless. Nevertheless since we are considering here only the dilute limit in which the driving field for the induced currents comes solely from the incident beam, we can take $\mathbf{B} \approx \mu_0\mathbf{H}$ and replace $\chi_{S\perp}^B \to \chi^H d/\mu_0$. We now substitute the replacements in relations (34)–(36) into Eq. (33) and compare it with Eqs. (15) and (16) to yield

$$\chi^E + \chi^H\cos^2\theta_i + \chi^H\sin^2\theta_i = 2i\gamma S(0), \tag{37}$$

$$\chi^E - \chi^H\cos^2\theta_i + \chi^H\sin^2\theta_i = 2i\gamma S_1(\pi - 2\theta_i)\frac{\sin k_z^i d}{k_z^i d}, \tag{38}$$

where we have assumed that the slab thickness d, where the centers of the randomly located spheres lie, is such that $k_z^i d \ll 1$; thus we can approximate in Eq. (16) $\sin k_z^i d/k_z^i d \approx 1$. We now solve Eqs. (37) and (38) for χ^E and χ^H and use the definitions of the electrical permittivity $\tilde{\epsilon} \equiv \epsilon/\epsilon_0 = 1 + \chi^E$ and the magnetic permeability $\tilde{\mu} \equiv \mu/\mu_0 = 1 + \chi^H$ to get

$$\tilde{\mu}_{\text{eff}}^{\text{TE}}(\theta_i) = 1 + i\gamma\frac{S_-^{(1)}(\theta_i)}{\cos^2\theta_i}, \tag{39}$$

$$\tilde{\epsilon}_{\text{eff}}^{\text{TE}}(\theta_i) = 1 + i\gamma[2S_+^{(1)}(\theta_i) - S_-^{(1)}(\theta_i)\tan^2(\theta_i)], \tag{40}$$

where

$$S_+^{(m)}(\theta_i) \equiv \tfrac{1}{2}[S(0) + S_m(\pi - 2\theta_i)], \tag{41}$$

$$S_-^{(m)}(\theta_i) \equiv S(0) - S_m(\pi - 2\theta_i), \tag{42}$$

and we have added to $\tilde{\epsilon}$ and $\tilde{\mu}$ the superindex TE to denote the polarization and the subindex eff to emphasize the fact that they describe an effective response.

In the case of TM polarization one performs a procedure analogous to the one developed for TE polarization, and one can show that the corresponding optical coefficients are given by

$$\tilde{\epsilon}_{\text{eff}}^{\text{TM}}(\theta_i) = 1 + i\gamma\frac{S_-^{(2)}(\theta_i)}{\cos^2\theta_i}, \tag{43}$$

$$\tilde{\mu}_{\text{eff}}^{\text{TM}}(\theta_i) = 1 + i\gamma[2S_+^{(2)}(\theta_i) - S_-^{(2)}(\theta_i)\tan^2(\theta_i)]. \tag{44}$$

These results can also be readily obtained from the symmetry in Maxwell's equations (the field-equivalence principle) and the results for TE polarization. That is, one replaces $\mathbf{E} \to -\mathbf{H}$ and $\epsilon \to \mu$. However, in doing so we must also replace the scattering matrix element $S_1(\pi - 2\theta_i) \to S_2(\pi - 2\theta_i)$.

Note that the effective optical coefficients $\tilde{\epsilon}_{\rm eff}$ and $\tilde{\mu}_{\rm eff}$ depend on the angle of incidence and on the polarization, and therefore they are not unrestricted. They are restricted to the slab geometry. Also the expressions for the effective optical coefficients in Eqs. (39)–(44) are linear in $\gamma \equiv 3f/2x^3$ and they are valid only to linear order in γ. This is consistent with the dilute-limit approximation adopted above, and therefore the validity of all of our results will be limited by this restriction.

According to CE the effective index of refraction $n_{\rm eff}$ should be given by

$$n_{\rm eff}^{(m)}(\theta_i) = [\tilde{\epsilon}_{\rm eff}^{(m)}(\theta_i)\tilde{\mu}_{\rm eff}^{(m)}(\theta_i)]^{1/2} \tag{45}$$

$$= \left\{1 + 2i\gamma S(0) - \frac{\gamma^2}{\cos^2\theta_i}[S(0)^2 - S_m(\pi - 2\theta_i)^2]\right\}^{1/2}, \tag{46}$$

and to lowest order in γ, one gets

$$n_{\rm eff} \approx 1 + i\gamma S(0), \tag{47}$$

which is isotropic and independent of polarization, and is actually the same result as that proposed by van de Hulst[9] and derived by Foldy[23] decades ago. So we can see that although the optical coefficients $\tilde{\epsilon}_{\rm eff}$ and $\tilde{\mu}_{\rm eff}$ are highly anisotropic and polarization-dependent, their dependence on the angle of incidence is such that the square root of their product is not.

Let us now look at some limiting cases. First we note that for small particles ($x \ll 1$) the Mie forward–backward anisotropy in the angular distribution of scattered radiation becomes

$$S_1(\theta_i) \approx -ix^3\beta, \tag{48}$$

$$S_2(\theta_i) \approx -ix^3\beta\cos\theta_i, \tag{49}$$

where $\beta = (\tilde{\epsilon}_S - 1)/(\tilde{\epsilon}_S + 2)$ and $\tilde{\epsilon}_S = \epsilon_S/\epsilon_0$ is the electrical permittivity of the spheres. Then $S_+^{(1)} \approx -ix^3\beta$, $S_-^{(1)} \approx 0$, $S_+^{(2)} \approx -ix^3\beta\sin^2\theta_i$, and $S_-^{(2)} \approx -2ix^3\beta\cos^2\theta_i$. Substituting these values into Eqs. (39)–(44) we get

$$\tilde{\mu}_{\rm eff}^{\rm TE}(\theta_i) = \tilde{\mu}_{\rm eff}^{\rm TM}(\theta_i) \equiv \tilde{\mu}_{\rm eff} = 1, \tag{50}$$

$$\tilde{\epsilon}_{\rm eff}^{\rm TE}(\theta_i) = \tilde{\epsilon}_{\rm eff}^{\rm TM}(\theta_i) \equiv \tilde{\epsilon}_{\rm eff} = 1 + 3\beta f. \tag{51}$$

These are the well-known results for the case of small particles, or for the case of an ordinary material when one regards the material as a composite made of molecular inclusions in vacuum. Eq. (50) tells us that the system is nonmagnetic and Eq. (51) is the low-density limit of the effective dielectric response in the Maxwell Garnett theory or in the Clausius–Mossotti relation, when one interprets β as proportional to the molecular polarizability. One can also see that the magnetic character of the system appears only when the spheres are large enough and is related to the large forward–backward anisotropy in the Mie scattering of large particles ($x \sim 1$).

For normal incidence ($\theta_i = 0$) one gets

$$\tilde{\mu}_{\rm eff}^{\rm TE}(0) = \tilde{\mu}_{\rm eff}^{\rm TM}(0) \equiv \tilde{\mu}_{\rm eff}(0) = 1 + i\gamma[S(0) - S_1(\pi)], \tag{52}$$

$$\tilde{\epsilon}_{\rm eff}^{\rm TE}(0) = \tilde{\epsilon}_{\rm eff}^{\rm TM}(0) \equiv \tilde{\epsilon}_{\rm eff}(0) = 1 + i\gamma[S(0) + S_1(\pi)], \tag{53}$$

where we have used $S_1(\pi) = -S_2(\pi)$. These are the expressions proposed by Bohren[16] when he introduced the idea of a magnetic response in the optical properties of granular materials made of nonmagnetic components.

At grazing incidence $\theta_i \to \pi/2$ we have that $S_m(\pi - 2\theta_i) \to S(0)$, thus $S_+^{(m)}(\theta_i) \to S(0)$ and $S_-^{(m)}(\theta_i) \to 0$ but $S_-^{(m)}(\theta_i)/\cos^2\theta_i$ remains finite. We can see this by expanding $S_-^{(m)}(\theta_i)$ around $\theta_i = \pi/2$ and showing that $\lim_{\theta_i\to\pi/2} S_-^{(m)}(\theta_i)/\cos^2\theta_i = 2S_m''(0)$ where the primes indicate the derivative with respect to the argument.

Now we illustrate the behavior of the effective optical coefficients of a random ensemble of spherical particles by performing some numerical calculations using the formulas derived above. The scattering matrix elements S_1 and S_2 are calculated following the recipe given in the book by Bohren and Huffman.[10] We choose an ensemble of nonabsorbing, nonmagnetic glass spheres with a real index of refraction $n_p = 1.50$. However, the formulas derived above and the evaluation of the elements of the scattering matrix are also valid when the spheres are magnetic or have a complex index of refraction. In the following figures we plot the change in the optical coefficients resulting from the presence of the spheres divided by the filling fraction of the spheres f. We may refer to these quantities as the normalized changes of the optical coefficients. We must remember that the present results are valid only for dilute systems, i.e., for $f \ll 1$.

In Fig. 2 we plot the normalized change in the real (a) and imaginary part (b) of the effective index of refraction given by Eq. (47) as a function of the ratio of the particle radius to the wavelength of the incident radiation. As can be appreciated in Fig. 2(a) the change in the real part starts increasing, reaches a maximum near 0.3 λ, and then drops rapidly and oscillates about $\mathrm{Re}(n_{\rm eff}) = 1$. Note that the contribution of the spheres to the real part of the refractive index can be negative, meaning that $n_{\rm eff}$ can be less than one. It is clear that for spheres larger than about 2λ their contribution to the effective index of refraction is rather small. In Fig. 2(b) we can see that the imaginary part has a strong peak at $a \sim 0.5\lambda$. Above $a = 1.0\lambda$, $\mathrm{Im}(n_{\rm eff})/f$ decreases slowly with some oscillations. Let us recall that since there is no absorption in the spheres, the imaginary part here means that the coherent field is lost due to diffuse scattering. Also, a small imaginary part of $n_{\rm eff}$ can have a significant effect. For example for $\mathrm{Im}(n_{\rm eff}) \simeq 0.01$ and for a wavelength of $\lambda = 0.55\,\mu$m the extinction coefficient becomes $2.3 \times 10^3\ \mathrm{cm}^{-1}$. The ripples (rapid oscillations) observed in both plots are the result of sphere resonances. However, when the spheres are not monodisperse the ripples tend to disappear. Note that $\mathrm{Im}(n_{\rm eff})$ remains positive for all particle radii, as it should. In Figs. 3(a)–3(d) we plot the normalized change in the effective electric permittivity and effective magnetic permeability given by Eqs. (39)–(44) as a function of the particle radius divided by the incident wavelength. As noted above, these effective opti-

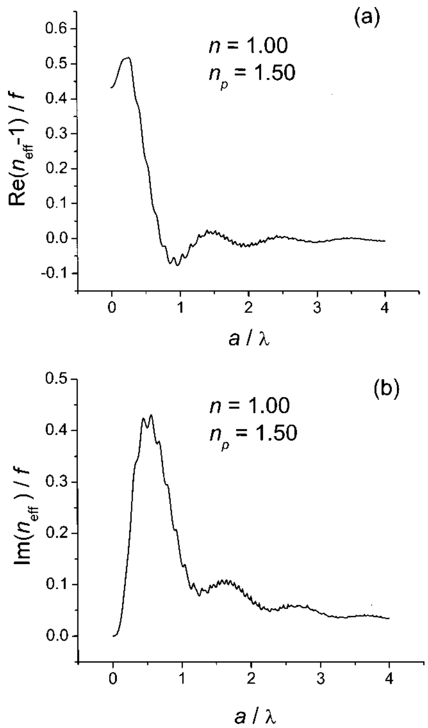

Fig. 2. Plots of the normalized change in the real and imaginary part of the effective index of refraction [Eq. (47)] as a function of a/λ for a system of nonmagnetic glass spheres ($n_p = 1.50$) in vacuum ($n = 1.00$).

cal coefficients depend on the angle of incidence. Thus we show plots for two different angles of incidence, $\theta_i = 30°$ and $\theta_i = 70°$. We may note that the behavior of the optical coefficients as a function of a/λ changes strongly from $\theta_i = 30°$ to $\theta_i = 70°$. In particular note that the maxima and minima in the plots for $\theta_i = 70°$ are larger than for $\theta_i = 30°$, and that the imaginary parts of $\epsilon_{\text{eff}}^{\text{TE}}$ and $\mu_{\text{eff}}^{\text{TM}}$ are negative above $a \simeq 0.4\lambda$ for $\theta_i = 70°$. This at first may seem troublesome, but for each polarization the sum of the imaginary parts of the effective optical coefficients ϵ_{eff} and μ_{eff} remains positive for all cases. In Figs. 4(a) and 4(b) we plot the normalized change in the real and imaginary parts of ϵ_{eff} and μ_{eff} for both polarizations as a function of the angle of incidence for a particle radius of $a = 0.5\lambda$. One can see the strong change in the optical coefficients towards grazing incidence. Here again even though $\operatorname{Im} \epsilon_{\text{eff}}^{\text{TE}}/f$ and $\operatorname{Im} \mu_{\text{eff}}^{\text{TM}}/f$ each negative values, we see that $\operatorname{Im} \epsilon_{\text{eff}}^{\text{TE}}/f + \operatorname{Im} \mu_{\text{eff}}^{\text{TE}}/f > 1$ and $\operatorname{Im} \epsilon_{\text{eff}}^{\text{TM}}/f + \operatorname{Im} \mu_{\text{eff}}^{\text{TM}}/f > 1$.

4. COHERENT REFLECTION AND TRANSMISSION FROM A HALF-SPACE

The coherent reflection from a half-space can be obtained by calculating the reflection amplitude from a semi-infinite pile of thin slabs of width d. If the slabs are thin enough ($k_z^i d \ll 1$) each slab may be modeled as an equivalent 2D sheet. Then the half-space becomes an in-

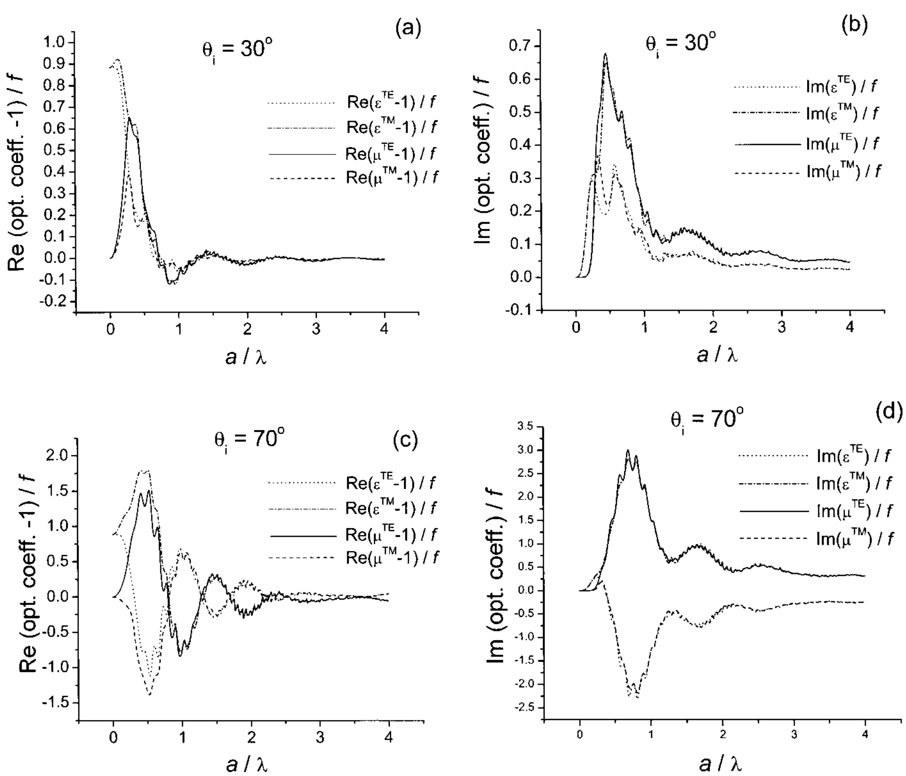

Fig. 3. Plots of the normalized change in the real (a), (c), and imaginary (b), (d) part of the optical coefficients [Eqs. (39)–(44)] as a function of the particle radius a divided by the wavelength λ, for two different angles of incidence, 30° (a), (b) and 70° (c), (d). The subindex eff in the optical coefficients was removed here for clarity. The plots are for a system of nonmagnetic glass spheres ($n_p = 1.50$) in vacuum ($n = 1.00$); dotted curves are for ϵ^{TE}, dashed-dotted curves for ϵ^{TM}, solid curves for μ^{TE}, and dashed curves for μ^{TM}.

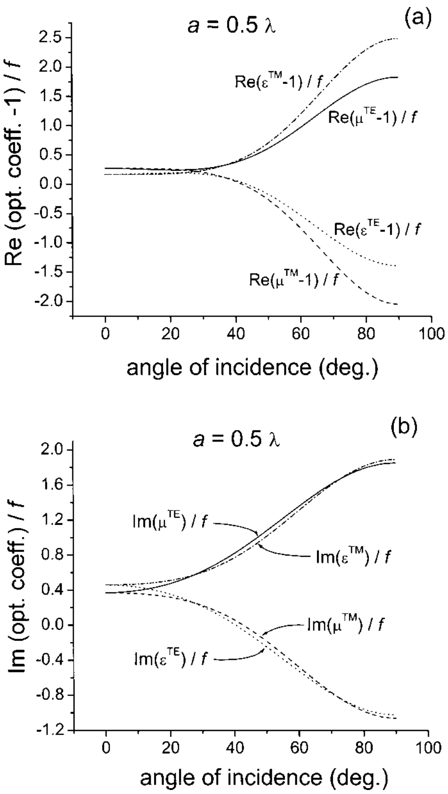

Fig. 4. Plots of the normalized change in the real (a) and imaginary (b) part of the optical coefficients [Eqs. (39)–(44)] as a function of the angle of incidence for particles of radius $a = 0.5\lambda$. The plots are for a system of nonmagnetic glass spheres ($n_p = 1.50$) in vacuum ($n = 1.00$). The subindex eff in the optical coefficients was removed here for clarity. Dotted curves are for ϵ^{TE}, dashed-dotted curves for ϵ^{TM}, solid curves for μ^{TE}, and dashed curves for μ^{TM}.

finite stack of sheets separated by a distance d and extending to the right of $z = 0$. This is illustrated in Fig. 5. A wave incoming to the half-space gets multiply scattered within the pile of sheets; the reflected wave is the sum of

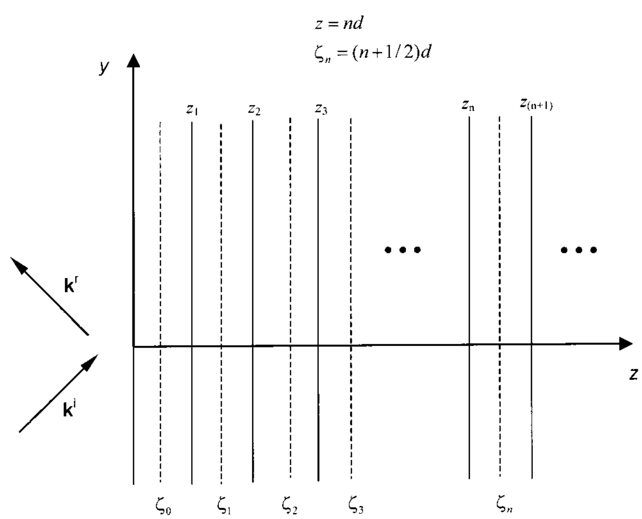

Fig. 5. Model of a half-space as a semi-infinite stack of 2D sheets. The sheets are located at $z = z_n = nd$ with $n = 0, 1, 2, 3, \ldots$. The fields are calculated at the intermediate planes $z = \zeta_n = (n + 1/2)d$.

the waves scattered to the left by all the sheets. To solve this multiple-scattering problem we consider only the field at planes lying halfway between the sheets, i.e., at the planes $z = \zeta_n = (n + 1/2)d$ with $n = 0, 1, 2, 3, \ldots$ (see Fig. 5). We then establish two coupled, multiple-scattering equations that relate the field between a pair of sheets to the field between all the other sheets. The solution for $z > 0$ is a right-propagating field with an envelope function $E_0 \exp(ik_z^{\mathrm{eff}} \zeta_n)$ and a left-propagating wave with an envelope function $r_{\mathrm{hs}} E_0 \exp(ik_z^{\mathrm{eff}} \zeta_n)$. The coefficient r_{hs} is the half-space reflection coefficient and k_z^{eff} is the z component of the effective propagation vector k^{eff}. The details of this procedure are given in Appendix A. In common materials the system of stacking sheets has been ordinarily used to illustrate the main ingredients present in a microscopic derivation of Fresnel's reflection formulas, as well as the physics behind the Ewald–Oseen extinction theorem. The effective propagation wave vector k^{eff} found through this procedure is the same as the one obtained above with the effective-medium approach [Eq. (47)]; the half-space TE reflection coefficient found with this procedure is

$$r_{\mathrm{hs}}^{\mathrm{TE}} = \frac{\gamma S_1(\pi - 2\theta_i)/\cos\theta_i}{i\{\cos\theta_i + [\cos^2\theta_i + 2i\gamma S(0)]^{1/2}\} - \gamma S(0)/\cos\theta_i}. \tag{54}$$

For TM polarization one finds the same expression but with $S_2(\pi - 2\theta_i)$ instead of $S_1(\pi - 2\theta_i)$. We must note that while for the scattering from each individual 2D sheet we use the single-scattering approximation, in obtaining the reflected field we take into account the multiple scattering between the sheets.

If we now accept the description of the optical properties of a granular material in terms of the effective optical coefficients given by Eqs. (39)–(44), the reflection amplitudes of a half-space r_{hs} must be given by the Fresnel relations of CE, that is,

$$r_{\mathrm{hs}}^{\mathrm{TE}} = \frac{\tilde{\mu}_{\mathrm{eff}}^{\mathrm{TE}}(\theta_i)k_z^i - k_z^{\mathrm{eff}}}{\tilde{\mu}_{\mathrm{eff}}^{\mathrm{TE}}(\theta_i)k_z^i + k_z^{\mathrm{eff}}}, \tag{55}$$

$$r_{\mathrm{hs}}^{\mathrm{TE}} = \frac{\tilde{\epsilon}_{\mathrm{eff}}^{\mathrm{TM}}(\theta_i)k_z^i - k_z^{\mathrm{eff}}}{\tilde{\epsilon}_{\mathrm{eff}}^{\mathrm{TM}}(\theta_i)k_z^i + k_z^{\mathrm{eff}}}, \tag{56}$$

where $k_z^{\mathrm{eff}} = k[(n^{\mathrm{eff}})^2 - \sin^2\theta_i]^{1/2}$ and $n^{\mathrm{eff}} = 1 + i\gamma S(0)$. It is not difficult to show that these Fresnel reflection coefficients obtained with the effective-medium theory coincide with Eq. (54) to first order in the density of particles. Consider for example TE polarization. The proof requires substituting Eqs. (39) and (40) into Eq. (55) and then multiplying the numerator and denominator by $ik^{-2}[\cos\theta_i + i\gamma S_-^{(1)}(\theta_i)/\cos\theta_i]^{-1}$ times the denominator. After dropping terms of second order in γ one arrives at Eq. (54). Here we must recall that $S_-^{(1)}(\theta_i)/\cos\theta_i \to 0$ at grazing incidence. The proof for TM polarization follows the same steps but $S_-^{(1)}(\theta_i)$ is replaced by $S_-^{(2)}(\theta_i)$.

Now one can see that the reflection coefficients of Eqs. (55) and (56) look very different from the ones we would have used by assuming that a nonmagnetic effective medium with $\tilde{\epsilon}_{\mathrm{eff}} = n_{\mathrm{eff}}^2 = [1 + i\gamma S(0)]^2$ and $\tilde{\mu}_{\mathrm{eff}} = 1$ is unrestricted, that is,

$$r_{\rm nm}^{\rm TE} = \frac{k_z^i - k_z^{\rm eff}}{k_z^i + k_z^{\rm eff}}, \qquad r_{\rm nm}^{\rm TM} = \frac{n_{\rm eff}{}^2 k_z^i - k_z^{\rm eff}}{n_{\rm eff}{}^2 k_z^i + k_z^{\rm eff}}, \tag{57}$$

where the subscript nm stands for nonmagnetic.

For the case of a slab with an arbitrary thickness h, the reflection r_h and transmission t_h amplitudes are given in terms of $r_{\rm hs}$ by the well-known expressions of CE, that is,

$$r_h = \frac{r_{\rm hs}[1 - \exp(2ik_z^{\rm eff}h)]}{1 - r_{\rm hs}{}^2 \exp(2ik_z^{\rm eff}h)}, \tag{58}$$

$$t_h = \frac{1 - r_{\rm hs}{}^2}{1 - r_{\rm hs}{}^2 \exp(2ik_z^{\rm eff}h)} \times \exp[-i(k_z^i - k_z^{\rm eff})h]. \tag{59}$$

These formulas are generally valid for both polarizations (TE and TM) yielding r_h and t_h in terms of the reflection amplitude of a half-space $r_{\rm hs}$ with the polarization corresponding to the ones given by Eqs. (55) and (56).

Up to now we have assumed that the spherical particles in the system are in vacuum. Extension of the above results to a lossless, homogeneous matrix with spherical inclusions is not difficult. We could start by considering an infinite medium with optical coefficients ϵ_m and μ_m (the subindex stands for matrix). Then we should use $\epsilon_m \epsilon_0$ and $\mu_m \mu_0$ instead of ϵ_0 and μ_0 throughout. In this case we should replace k by $n_m k$ with $n_m = (\epsilon_m \mu_m)^{1/2}$, where n_m is real since we are assuming a lossless medium. For example we should now use $x = n_m ka$ instead of $x = ka$. Then we consider the reflection and transmission from a thin slab of spherical inclusions within the matrix as light coming from the matrix alone. The components of the scattering matrix should be evaluated with the sphere embedded in a medium with optical coefficients ϵ_m and μ_m. The angle of travel inside the matrix is different from the angle outside the matrix because of refraction at the air–matrix interface. We will denote by θ_m the angle of travel inside the matrix assuming that before entering (or leaving) the matrix the angle is θ_i, and θ_i and θ_m are related by Snell's law. Now we denote with $r'_{\rm hs}$ the reflection amplitude at the interface between the homogeneous matrix and the composite matrix with spherical inclusions, and it will be given by Eqs. (55) and (56) with the replacements mentioned above, that is, $k \to n_m k$, $\theta_i \to \theta_m$, and the components of the scattering matrix calculated with the sphere embedded in the matrix. For example, $k_z^{\rm eff}$ will now be given by $k_z^{\rm eff} = k[(n_{\rm eff})^2 - n_m^2 \sin^2 \theta_m]^{1/2}$. With these considerations, formulas (39)–(44) will yield $\epsilon_{\rm eff}/\epsilon_m$ and $\mu_{\rm eff}/\mu_m$ for the corresponding polarization.

The coherent-reflection amplitude from a half-space of the composite-matrix material $r_{\rm cm}$ is obtained by calculating the reflection from the system *vacuum–homogeneous matrix–composite matrix*. This corresponds to a thin slab of *homogeneous matrix* on a *composite-matrix* substrate. The reflection coefficient is

$$r_{\rm cm} = \frac{r_m + r'_{\rm hs} \exp(2ikn_m \cos\theta_m g)}{1 + r_m r'_{\rm hs} \exp(2ikn_m \cos\theta_m g)}, \tag{60}$$

where r_m is the reflection coefficient of the *vacuum–homogeneous-matrix* interface and g is the width of the *homogeneous-matrix* slab. If we assume that all the particles are entirely embedded in the matrix, we cannot let $g \to 0$; we must at least take g equal to the radius a of the particles. Here r_m may include the effects of roughness at the matrix interface whenever this might be important, and g could be adjusted to accommodate for some other boundary condition related to the density of particles. In an experimental situation the particles will be immersed in a matrix. For dilute systems of particles, the contribution of the particles to the coherent reflectance will generally be small compared to that of the matrix–vacuum interface except near grazing incidence. If one intended to detect the contribution of the particles to the coherent reflectance, one might need to use differential measurements, such as the difference between the reflectance for two orthogonally polarized incident beams, or an ellipsometric technique. Other possibilities are to suppress the reflection from the matrix–vacuum interface by taking advantage of the Brewster-angle effect, or by using the critical-angle effect, which is in a way equivalent to measuring the reflectance associated with the particles near grazing incidence.

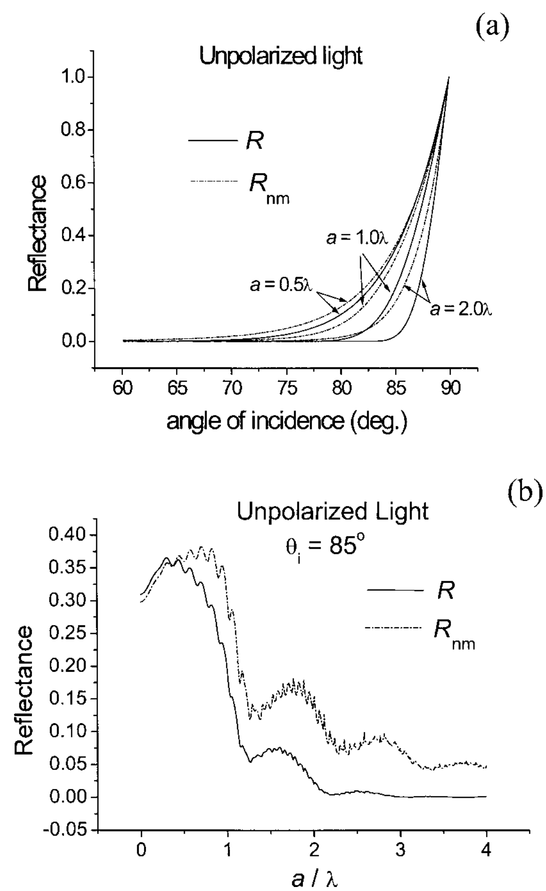

Fig. 6. Plot of the coherent reflectance R of unpolarized light [average of Eqs. (55), (56)] for a system of nonmagnetic glass spheres ($n_p = 1.50$) in vacuum ($n = 1.00$) with a filling fraction of $f = 0.1$; (a) as a function of the angle of incidence and for several values of the radius a of the particles, (b) as a function of the particle radius a divided by the wavelength λ for an angle of incidence $\theta_i = 85°$. For comparison we also plot the reflectance ignoring the effective magnetic susceptibility [$R_{\rm nm}$ from Eq. (57)].

Now we show some numerical results and some comparisons between the results of Eqs. (55) and (56) and those corresponding to the nonmagnetic effective medium given by Eq. (57). We choose the same parameters as in the illustrative example presented above of nonmagnetic, transparent, glass particles. In Fig. 6(a) we plot the coherent-wave reflectance from Eqs. (55) and (56) for unpolarized light, i.e., $\frac{1}{2}|r_{\mathrm{hs}}^{\mathrm{TE}}|^2 + \frac{1}{2}|r_{\mathrm{hs}}^{\mathrm{TM}}|^2$ as a function of the angle of incidence for several values of the particle radius and a filling fraction of $f = 0.1$. The reflectance calculated by using the Fresnel relations corresponding to a nonmagnetic effective medium [Eq. (57)] is also shown. In Fig. 6(b) we plot the coherent reflectance for unpolarized light as a function of the particle radius divided by λ for an angle of incidence of 85°. At this angle of incidence the coherent reflectance is large enough to be measured easily. Also for comparison we show the nonmagnetic reflectance. Both Figs. 6(a) and 6(b) clearly show that if one ignores the effective magnetic susceptibility in Fresnel relations, one overestimates considerably the coherent reflectance. For angles of incidence away from grazing incidence there are some interesting features of the reflectance that it is worthwhile to point out. In Fig. 7(a) we show the TM-polarized reflectance near the Brewster angle for particles with radius of $a = 0.2\lambda$. It can be seen that the Brewster angle predicted by the nonmagnetic reflectance differs from our result by a few degrees. In Fig. 7(b) we show the reflectance for TE polarization in an amplified scale for intermediate angles of incidence. It can be appreciated that the reflectance has two zeros, and these are the zeros of the scattering matrix element S_1. These zeros could be interpreted as Brewster angles showing the need for having a magnetic permeability in the effective medium, since only magnetic materials manifest a Brewster angle in TE polarization.

Considering the validity of our results, one can assert that the formulas derived here are strictly valid only for point-Mie scatterers and become exact only in the dilute limit. However, it is possible to use our formulas for a small but finite concentration of Mie scatterers with finite radius. The limits of validity should be determined in terms of a/λ, θ_i, and f. Although these limits should be set through the comparison of our results with those obtained with more elaborate approximations, at the moment we may use the second-order terms which were dropped in our formulas as an indication of the confidence in the calculated parameters. For example if we had not dropped second-order terms in our procedure, we would have obtained the half-space reflection coefficient as

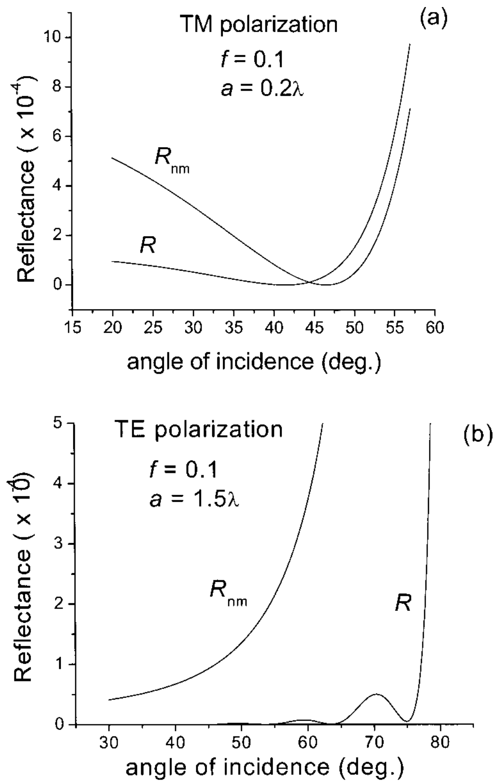

Fig. 7. Interesting features of the coherent reflectance R as a function of the angle of incidence for a system of nonmagnetic glass spheres ($n_p = 1.50$) in vacuum ($n = 1.00$) with a filling fraction of $f = 0.1$. (a) Brewster's angle for TM polarization [Eq. (56)] for particles of radius $a = 0.2\lambda$, (b) Brewster's angle for TE polarization for particles of radius $a = 1.5\lambda$. For comparison we also plot the reflectance ignoring the effective magnetic susceptibility [$R_{\mathrm{n\text{-}m}}$ from Eq. (57)].

show that E is largest within a window of angles of incidence from about 80° to 89°. For particles of radius up to $a = 4\lambda$, we find that for a filling fraction of $f = 0.1$, E is always less than 0.17. For a filling fraction of $f = 0.05$, E is always less than 0.10 and for a filling fraction of $f = 0.01$, E is always less than 0.016. Outside the 80°–89° window, E is always smaller than the numbers just quoted. For example, at 70° the largest value of E for $f = 0.1$ is found to be 0.037 for particles of radius near $a = 0.7\lambda$; at 89.9° and also for $f = 0.1$, E is found to increase monotonically (with some ripple structure) with increasing particle radius, reaching 0.037 at $a = 4\lambda$. This might mean that the coherent reflectance given by Eqs. (55) and (56) or by Eq. (54) is more strongly limited in

$$r_{\mathrm{hs}} = \frac{\gamma S_m(\pi - 2\theta_i)/\cos\theta_i}{i(\cos\theta_i + \{\cos^2\theta_i + 2i\gamma S(0) - (\gamma^2/\cos^2\theta_i)[S(0)^2 - S_m(\pi - 2\theta_i)^2]\}^{1/2}) - \gamma S(0)/\cos\theta_i}, \tag{61}$$

where $m = 1, 2$ for TE and TM polarization, respectively. Then a measure of the possible error would be $E \equiv |R - R_{\mathrm{so}}|/R$, where R and R_{so} are the modulus squared of Eqs. (54) and (61), respectively.

Numerical calculations considering glass particles terms of the filling fraction for angles of incidence within some range near grazing incidence than near normal incidence; and that apparently—very close to grazing (a few tenths of a degree)—the accuracy improves again as long as the particles are not too large.

Further comments about the reflection coefficient near grazing incidence are worth making at this point. The formulas for the coherent reflection coefficient r_{hs} given above approach the value of -1 as $\theta_i \to \pi/2$ (grazing), which is the correct result. Although our approximations to the optical coefficients are to first order in the filling fraction, the z-component of the propagation vector appears in the expression for r_{hs}. This component can be written as $k_z^{\mathrm{eff}} = k[\cos^2\theta_i + 2i\gamma S(0)]^{1/2}$. Now we cannot expand this expression in powers of γ and drop the second- and higher-order terms because at grazing incidence $\cos\theta_i \to 0$ and we are left with a term of order $(\gamma)^{1/2}$ which is larger than γ for $\gamma < 1$. Also the reflection coefficient is given as the ratio of two expressions. We may neglect second- and higher-order powers of γ in the numerator and denominator, but we cannot expand the quotient in powers of γ, truncate the series, and take the limit of grazing incidence, again because $\cos\theta_i$ approaches zero as $\theta_i \to \pi/2$. Thus the reflection coefficient near grazing incidence contains terms with all powers of γ. The second- and higher-order terms are incomplete, but we believe that the most important parts of these terms are included in the approximation for dilute systems.

5. DISCUSSION AND CONCLUSIONS

Using wave-scattering theory, we calculated the coherent reflectance of electromagnetic radiation from a half-space filled with randomly located, polarizable spheres at an arbitrary angle of incidence. Our results are valid in the dilute limit since the effects of multiple scattering have been included only in an average sense. As a matter of fact, it can be shown[27] that our approximation is formally equivalent to the well-known effective-field approximation used in electromagnetic wave theory of multiple scattering.[23–25] As another objective of our work we looked at the relation of our results to those of an effective-medium approach. The concept of an effective medium in a granular system when the size of the inclusions is comparable to the wavelength of the incident radiation has been rather elusive. Here we give a precise definition of its meaning in relation to the propagation, reflection, and transmission of the average (coherent) electromagnetic field. We have found that the effective index of refraction derived within this approximation or equivalently derived in a more intuitive way by van de Hulst[9] cannot be regarded as unrestricted. That is it cannot be safely used in CE as if it were the refractive index of a homogeneous material. This does not mean that the concept of an effective refractive index is not meaningful in this case. On the contrary, if one wants to look at the system as an effective medium, we show that a proper and accurate description of the coherent reflectance from the half-space system requires an independent determination of the effective electric permittivity and the effective magnetic permeability of the system. We provide explicit expressions for these optical coefficients in terms of the elements of the scattering matrix of the isolated sphere as well as for the reflection amplitude of a half-space for both polarizations of the incident beam. It turns out that the effective optical coefficients depend not only on the polarization of the incident beam but also on the angle of incidence. Thus they cannot be regarded as unrestricted but rather as restricted to the slab geometry. The possibility of constructing unrestricted optical coefficients for this system is still an open question.

Nonetheless we believe that the expressions derived here, although limited to dilute systems, are not purely and simply a curiosity, but on the contrary they may be useful in several applications. For example, there is now interest in following in real time various processes that take place in turbid media through the changes in their effective index of refraction. Nevertheless although measurements of the attenuation of light through turbid systems are done routinely in many laboratories, there are few transmission experiments which measure both the real and imaginary part of their effective index of refraction.[21,28] However, a simple and potentially very useful way of measuring the effective index of refraction in turbid media is by critical-angle refractometers.[29–31] In this method the real and imaginary parts of the effective index of refraction are obtained by inverting the relationship between the reflection amplitude and the effective index of refraction. The naive use of Fresnel expressions to perform this inversion would lead to errors in both accuracy and interpretation. However, the expressions for the reflection amplitude derived here could be used, together with data of critical-angle refractometers, to obtain not only more accurate results of the optical constants of turbid media, but to undertake reliable modeling of the correlation between their changes and some of the specific processes which take place within the system.

In radiative-transfer studies in granular matter the calculation of the internal and external reflectance of the energy fluxes at the boundaries requires knowledge of the index of refraction of the matrix; in its absence these reflectances are usually set equal to zero. Since radiative-transfer theories are based on the balance of fluxes, they cannot account for interference phenomena such as coherent reflectance. However, one could take it into account by regarding the system as an effective medium and using the formulas derived here for the calculation of the internal and external reflectance. In this way we provide a solid justification for earlier suggestions[32] along these lines.

Another consequence of our results is knowledge of the existence of an effective magnetic permeability (different from that in vacuum) in a system in which both the matrix and the inclusions are nonmagnetic. Although this idea has been put forward previously, the physical nature of this magnetic response was not clear and had even been regarded by some authors[17] as a purely mathematical construct rather than the actual manifestation of a physical phenomenon. In some respects our work can be regarded as an extension of Bohren's expressions in Ref. 16. One of our aims has also been to provide a clear physical picture of the nature of this magnetic response. To pursue that aim we have derived the optical coefficients by looking at the spatial distribution of the average currents induced by the applied field, and we have concluded that the magnetic response comes from the existence of induced closed currents. These average closed currents should be currents induced in the spheres by the time variations of the magnetic field, thus yielding a true magnetic response in the system. This mechanism of magnetic response is very similar to that proposed by Ampère in the early days of electrodynamics in which the closed currents were supposed to be induced in the molecules. A modern version of this type of Amperian magnetism can be found in the microstructured materials reported by Pendry *et al.*[33] for the microwave region. In these materials the closed currents are induced in small metallic rings of millimetric size disposed in a periodic structure and embedded in an insulating matrix. In this way the authors build a magnetic-microstructured material as a composite with nonmagnetic components. In a certain manner, the mechanism behind the magnetic response in these microstructured materials is analogous to the one found here for a system of randomly located spheres.

In conclusion although the approximation used in our calculations is rather simple, and it can be shown to be equivalent to the well-known effective-field approximation,[27] and although the structure of more sophisticated procedures has already been depicted,[22,26] the merits of our work are the following:

1. to derive expressions for the coherent-reflection coefficient of a half-space of a random system of Mie scatterers,
2. to derive explicit expressions for the effective optical coefficients and the reflection amplitude for a slab geometry and for an arbitrary angle of incidence, and
3. to establish that the magnetic response in a system with nonmagnetic components is a true magnetic response the result of induction of closed currents in the spherical inclusions.

Extensions of our results to random systems of spheres with a distribution either in size or in optical coefficients is straightforward and requires an averaging of the scattering-matrix elements over the distribution of sizes and indices of refraction. Extending the present formulation to more-densely-packed random systems by including local-field corrections will be explored in the near future.

APPENDIX A

In this appendix we derive the half-space reflection coefficient by regarding the system as a semi-infinite stack of thin slabs of width d separated by infinitesimal vacuum gaps. Between the slabs (free space) the field is given by right-propagating and left-propagating waves with wave vectors $\mathbf{k}^i$ and $\mathbf{k}^r$, respectively. The right-propagating wave has the same polarization as the incident field ($\hat{\mathbf{e}}_i$) while the left-propagating wave is polarized as the reflected field from the half-space ($\hat{\mathbf{e}}_r$). We now denote the amplitude of the scattered fields divided by the amplitude of the incident field times the width of the slab d as the scattering coefficients α and β. Each thin slab of width d is modeled as a 2D sheet (see Fig. 5). In the dilute random system of spheres when $k_z^i d \ll 1$, we have for TE polarization [see Eqs. (15) and (16)]

$$\alpha = -\gamma \frac{k}{\cos\theta_i} S(0), \tag{A1}$$

$$\beta = -\gamma \frac{k}{\cos\theta_i} S_1(\pi - 2\theta_i). \tag{A2}$$

For TM polarization, $S_1(\pi - 2\theta_i)$ in β is replaced by $S_2(\pi - 2\theta_i)$. Let us assume that the 2D sheets are located at $z = z_n = nd$ where $n = 0, 1, 2, 3\ldots$ as shown in Fig. 5. Our aim is to calculate the field between the sheets, that is, at locations $z = \zeta_n = (n + 1/2)d$. Let us denote the field at these planes by $\mathbf{E}_n = \mathbf{E}(z = \zeta_n)$ and write

$$\mathbf{E}_n = (E_n^+ \hat{\mathbf{e}}_i + E_n^- \hat{\mathbf{e}}_r)\exp(ik_x^i x + ik_y^i y), \tag{A3}$$

where E_n^+ and E_n^- are scalar functions giving the amplitudes and the z-dependence of the phase of the right- and left-propagating waves, respectively. Now the field at any plane is given by the incident field plus the scattered fields from all the 2D sheets. It is not difficult to show that the following equations hold:

$$E_n^+ = E_n^i + \sum_{m=0}^{n} (\beta E_m^- + \alpha E_{m-1}^+)\exp[ik_z^i(\zeta_n - z_m)]d, \tag{A4}$$

$$E_n^- = \sum_{m=n}^{\infty} (\beta E_m^+ + \alpha E_{m+1}^-)\exp[-ik_z^i(\zeta_n - z_{m+1})]d, \tag{A5}$$

where E_n^i is the corresponding scalar function of the incident field evaluated at $z = \zeta_n$. Given that we are already assuming $k_z^i d \ll 1$ we can approximate the above summations by integrals as

$$E^+(z) = E^i(z) + \int_0^z [\beta E^-(z') + \alpha E^+(z')] \times \exp[ik_z^i(z - z')]\mathrm{d}z', \tag{A6}$$

$$E^-(z) = \int_z^\infty [\beta E^+(z') + \alpha E^-(z')] \times \exp[-ik_z^i(z - z')]\mathrm{d}z'. \tag{A7}$$

Now for $z > 0$ one proposes the solution

$$E^+(z) = E_0 \exp(ik_z^{\mathrm{eff}} z), \tag{A8}$$

$$E^-(z) = r_{\mathrm{hs}} E_0 \exp(ik_z^{\mathrm{eff}} z), \tag{A9}$$

where k_z^{eff} is the z-component of an effective propagation wave vector and E_0 is the amplitude of the incident wave. Note that although microscopically the wave E^- travels to the left, the phase of the envelope function travels to the right. Since at $z = 0$ the reflected wave must match the wave traveling to the left (microscopically), the result is that r_{hs} is the half-space reflection coefficient. We may substitute Eq. (A8) and Eq. (A9) into the above integral equations and perform the integration. Assuming now that k_z^{eff} has a small nonzero imaginary part, we take $\exp(ik_z^{\mathrm{eff}} z)$ at $z = \infty$ equal to zero. In Eq. (A8), one must require that the incident field be canceled by one of the terms obtained from the integration (Ewald–Oseen theorem). From this we get

$$r_{\mathrm{hs}} = \frac{i(k_z^{\mathrm{eff}} - k_z^i) - \alpha}{\beta}, \tag{A10}$$

and from the second equation, we get

$$r_{\mathrm{hs}} = -\frac{\beta}{i(k_z^{\mathrm{eff}} + k_z^i) + \alpha}. \tag{A11}$$

Equating these two equations and solving for k_z^{eff} yields

$$k_z^{\mathrm{eff}} = [(k_z^i)^2 - 2ik_z^i\alpha + \beta^2 - \alpha^2]^{1/2}, \tag{A12}$$

which in turn may be used in either Eq. (A10) or Eq. (A11) for the half-space reflection coefficient. These are the results of a wave-scattering approach.

As a check it is not difficult to show that for a homogeneous medium, if one uses the appropriate scattering coefficients for thin slabs of width $d \ll 1/k_z^i$, one recovers the Fresnel reflection relations from either Eq. (A10) or Eq. (A11). Now if one uses the scattering coefficients in TE polarization for the dilute random system of spheres given in Eqs. (A1) and (A2) and drops terms of second order in γ one gets

$$k_z^{\mathrm{eff}} = k[\cos^2\theta_i + 2i\gamma S(0)]^{1/2} \tag{A13}$$

and

$$r_{\mathrm{hs}}^{\mathrm{TE}} = \frac{\gamma S_1(\pi - 2\theta_i)/\cos\theta_i}{i(\cos\theta_i + [\cos^2\theta_i + 2i\gamma S(0)]^{1/2}) - \gamma S(0)/\cos\theta_i}, \tag{A14}$$

where $k_z^i = k\cos\theta_i$ was used. For TM polarization one gets the same results but with $S_1(\pi - 2\theta_i)$ replaced by $S_2(\pi - 2\theta_i)$. The effective index of refraction can be obtained from Eq. (A13) by using $k_z^{\mathrm{eff}} = k(n_{\mathrm{eff}}^2 - \sin^2\theta_i)^{1/2}$. One gets

$$n_{\mathrm{eff}} = [1 + 2i\gamma S(0)]^{1/2} \approx 1 + i\gamma S(0), \tag{A15}$$

which coincides with the result obtained in Eq. (47) from the effective-medium approach.

ACKNOWLEDGMENTS

We acknowledge very fruitful and illuminating discussions with E. Méndez. The partial support of Consejo Nacional de Ciencia y Tecnología (México), Centro de Investigación en Polímeros (Grupo COMEX) through grant RI-1200-2-1, and the support of Dirección General de Personal Académico of Universidad Nacional Autónoma de México through grant IN-104201 are also acknowledged.

A. Garcia-Valenzuela may be reached by e-mail at garciaa@aleph.cinstrum.unam.mx.

REFERENCES

1. Lord Rayleigh, "On the transmission of light through an atmosphere containing small particles in suspension, and on the origin of the blue of the sky," Philos. Mag. **47**, 375–384 (1899).
2. R. Ruppin, "Evaluation of extended Maxwell Garnett theories," Opt. Commun. **182**, 273–279 (2000).
3. J. C. Maxwell Garnett, "Colours in metal glasses and in metallic films," Philos. Trans. R. Soc. London **203**, 385–420 (1904).
4. See, for example, the historical review of R. Landauer, "Electrical conductivity in inhomogeneous media," in *Proceedings of the First Conference on Electrical Transport and Optical Properties of Inhomogeneous Media*, J. C. Garland and D. B. Tanner, eds., American Institute of Physics Conf. Proc. No. 40 (American Institute of Physics, New York, 1978), pp. 2–45.
5. J. E. Gubernatis, "Scattering theory and effective medium approximation to heterogeneous materials," in *Proceedings of the First Conference on Electrical Transport and Optical Properties of Inhomogeneous Media*, J. C. Garland and D. B. Tanner, eds., American Institute of Physics Conf. Proc. No. 40 (American Institute of Physics, New York, 1978), pp. 84–97.
6. R. Fuchs, "Optical properties of small particle composites," in *Proceedings of the First Conference on Electrical Transport and Optical Properties of Inhomogeneous Media*, J. C. Garland and D. B. Tanner, eds., American Institute of Physics Conf. Proc. No. 40 (American Institute of Physics, New York, 1978), pp. 276–281.
7. For more recent references, see, for example, *Proceedings of the Fifth International Conference on Electrical Transport and Optical Properties of Inhomogeneous Media* (ETOPIM 5), P. M. Hui, P. Sheng, and L.-H. Tang, eds., Physica B **279**, Nos. 1–3 (2000).
8. D. A. G. Bruggeman, "Berechnung verschiedener physikalicher Konstanten von heterogenen Substanzen. I. Dielektrizitätkonstanten und Leitfähigkeiten der Mischkörper aus isotropen Substanzen," Ann. Phys. (Leipzig) **24**, 636–679 (1935).
9. H. C. van de Hulst, *Light Scattering by Small Particles* (Wiley, New York, 1957).
10. C. F. Bohren and D. R. Huffman, *Absorption and Scattering of Light by Small Particles* (Wiley, New York, 1983).
11. D. Stroud and F. P. Pan, "Self-consistent approach to electromagnetic wave propagation in composite media: application to model granular metals," Phys. Rev. B **17**, 1602–1610 (1978).
12. P. Chýlek and V. Srivastava, "Dielectric constant of a composite inhomogeneous medium," Phys. Rev. B **27**, 5098–5106 (1983).
13. W. T. Doyle, "Optical properties of a suspension of metal spheres," Phys. Rev. B **39**, 9852–9858 (1989).
14. A. Wachniewski and H. B. McClung, "New Approach to effective medium for composite materials: application to electromagnetic properties," Phys. Rev. B **33**, 8053–8059 (1986).
15. C. A. Grimes and D. M. Grimes, "Permeability and permittivity spectra of granular materials," Phys. Rev. B **43**, 10780–10788 (1991).
16. C. F. Bohren, "Applicability of effective medium theories to problems of scattering and absorption by nonhomogeneous atmospheric particles," J. Atmos. Sci. **43**, 468–475 (1986).
17. P. Chýlek, G. Videen, D. J. W. Geldart, J. S. Dobbie, and H. C. W. Tso, "Effective medium approximations for heterogeneous particles," in *Light Scattering by Nonspherical Particles*, M. I. Mishchenko, J. W. Hovenier, and L. D. Travis, eds. (Academic, New York, 2000), Chap. 9.
18. See for example, L. Tsang, J. A. Kong, and R. Shin, *Theory of Microwave Remote Sensing* (Wiley, New York, 1985).
19. L. Tsang and J. A. Kong, "Multiple scattering of electromagnetic waves by random distribution of discrete scatterers with coherent potential and quantum mechanical formalism," J. Appl. Phys. **51**, 3465–3485 (1980).
20. L. Tsang and J. A. Kong, "Effective propagation constants for coherent electromagnetic waves propagating in media embedded with dielectric scatterers," J. Appl. Phys. **53**, 7162–7173 (1982).
21. Y. Kuga, D. Rice, and R. D. West, "Propagation constant and the velocity of the coherent wave in a dense strongly scattering medium," IEEE Trans. Antennas Propag. **44**, 326–332 (1996).

22. V. A. Loiko, V. P. Dick, and A. P. Ivanov, "Features in coherent transmittance of a monolayer of particles," J. Opt. Soc. Am. A **17**, 2040–2045 (2000).
23. L. L. Foldy, "The multiple scattering of waves," Phys. Rev. **67**, 107–119 (1945).
24. M. Lax, "Multiple scattering of waves II. The effective field in dense systems," Phys. Rev. **85**, 621–629 (1952).
25. M. Lax, "Multiple scattering of waves," Rev. Mod. Phys. **23**, 287–310 (1951).
26. L. Tsang and J. A. Kong, *Scattering of Electromagnetic Waves; Advanced Topics* (Wiley, New York, 2001), Chap. 3, pp. 128–130.
27. A. García-Valenzuela and R. G. Barrera, "Electromagnetic response of a random half-space of Mie scatterers within the effective medium approximation and the determination of the effective optical coefficients," J. Quant. Spectrosc. Radiat. Transfer (to be published).
28. C. Yang, A. Wax, and M. S. Feld, "Measurement of the anomalous phase velocity of ballistic light in a random medium by use of a novel interferometer," Opt. Lett. **26**, 235–237 (2001).
29. G. H. Meeten and A. N. North, "Refractive index measurement of absorbing and turbid fluids by reflection near the critical angle," Meas. Sci. Technol. **6**, 214–221 (1995).
30. M. Mohammadi, "Colloidal refractometry: meaning and measurement of refractive index for dispersions; the science that time forgot," Adv. Colloid Interface Sci. **62**, 17–29 (1995).
31. A. García-Valenzuela, M. Peña-Gomar, and C. Fajardo-Lira, "Measuring and sensing a complex index of refraction by laser reflection near the critical angle," Opt. Eng. **41**, 1704–1716 (2002).
32. W. E. Vargas and G. A. Niklasson, "Applicability conditions of the Kubelka–Munk theory," Appl. Opt. **36**, 5580–5586 (1997).
33. J. B. Pendry, A. J. Holden, D. J. Robbins, and W. J. Stewart, "Magnetism from conductors, and enhanced nonlinear phenomena," IEEE Trans. Microwave Theory Tech. **47**, 2075–2084 (1999).